

## Young-Type Interference in ( $e, 2e$ ) Ionization of $H_2$

D. S. Milne-Brownlie,<sup>1</sup> M. Foster,<sup>2</sup> Junfang Gao,<sup>2</sup> B. Lohmann,<sup>1</sup> and D. H. Madison<sup>2</sup>

<sup>1</sup>*ARC Centre for Antimatter-Matter Studies, Griffith University, Nathan, QLD 4111 Australia*

<sup>2</sup>*Department of Physics, University of Missouri-Rolla, 1870 Miner Circle, Rolla, Missouri 065409, USA*

(Received 5 March 2006; published 14 June 2006)

We have investigated the electron impact single ionization of the hydrogen molecule, with fully determined kinematics. The experimental and theoretical results are compared with He ionization under the same conditions. The results indicate that the ejected electron angular distribution for  $H_2$  is modified due to Young-type interference between ionization amplitudes for scattering from the two centers in the hydrogen molecule. The observable result is a suppression of the backward scattering (recoil) peak compared with the binary peak.

DOI: [10.1103/PhysRevLett.96.233201](https://doi.org/10.1103/PhysRevLett.96.233201)

PACS numbers: 34.80.Dp

There has been considerable interest in recent years in the evidence for quantum mechanical interference effects in charged particle impact ionization of  $H_2$  molecules. This interference can be considered as a “Young-type” interference in which the two sources of coherent emission (the two slits) are the two atomic centers in the molecular target. Superposition of the ionization amplitudes from these two centers is expected to produce an interference pattern, with the features of the interference pattern depending upon the internuclear distance (the slit width) and the (emitted) electron wavelength. Such interference effects, arising from the interference of the amplitudes for ionization from the two, indistinguishable, hydrogen atoms, have been predicted theoretically [1]; the prediction is that energy-dependent or angle-dependent oscillations in the cross section may be observed, depending upon the type of measurement which is performed. Measurements of the double differential cross section (DDCS) for ionization of  $H_2$  by heavy ions [2–4], and by electrons (for  $D_2$ ) [5], have been reported. The results exhibit oscillatory structure, as a function of the emitted electron energy, which has been attributed to interference effects, with the results being in reasonable agreement with theoretical calculations. These studies were primarily directed at observing interference structures as a function of emitted electron energy, for fixed electron emission angles, with the scattering angle of the projectile being integrated over. If interference effects can be seen in the double differential cross sections, which integrate over the projectile scattering angle, then they might be more readily observable in experiments with fully determined kinematics for both the scattered projectile and ejected electron [1,6] since integrations can diminish (or even eliminate) interesting effects. The cross section measured in such a process (sometimes called the triple differential cross section, TDCS, or a fully differential cross section, FDCS) corresponds to the probability of detecting an ejected electron of given energy, as a function of angle, for specified energy and detection angle of the scattered electron. In the case of  $H_2$ , the theoretical results predict that measurable interference effects should be observable in the angular distribu-

tions of the ejected electron for a fixed projectile scattering angle (even for angle-averaged target orientations), but that experimental observation of the interference may require, as was the case for the previous DDCS measurements, the determination of the ratio between  $H_2$  and H cross sections, with the latter being generally theoretically predicted (only one experiment has been reported in which an experimental value for the H cross section was measured [5]). In effect, the molecular cross sections must be divided by a “single center” atomic cross section in order for the effect of interference to become visible. A similar approach was employed in recent work [7] in which experimental TDCS results for electron impact ionization of  $H_2$ , primarily in the coplanar symmetric kinematics, were presented, although no evidence was found for interference effects in the angular distribution.

In order to avoid relying solely on theoretical cross section values, we have investigated experimentally the behavior of the TDCS for electron impact ionization of  $H_2$ , in comparison with the TDCS for ionization of the comparable two-electron, single center target, i.e., the helium atom. The experimental data were obtained at an intermediate incident electron energy of 250 eV, using coplanar asymmetric kinematics, at several different ejected electron energies. It has been suggested [6] that interference effects are more likely to be observed in the asymmetric geometry. In coplanar asymmetric kinematics, the higher energy outgoing electron (identified as the scattered electron) is detected at a fixed forward angle, in our case  $-15^\circ$ . The lower energy outgoing electron (the ejected electron) is detected at various angles in the scattering plane. The energies of the ejected electrons detected in this work were 10, 20, and 50 eV. The energy of the scattered electron may be determined from energy conservation, such that

$$E_i = E_a + E_b + \varepsilon, \quad (1)$$

where  $E_i$  is the incident electron energy,  $E_a$  and  $E_b$  are the scattered and ejected electron energies, respectively, and  $\varepsilon$  is the binding energy of the particular orbital which is being ionized [24.5 eV for He and 15.4 eV for  $H_2$ ].

Under such conditions, the TDCS generally contains two structures, the forward angle “binary” peak, and the backward angle “recoil” peak. The former involves a direct knockout of the bound electron, while the recoil peak is due to a further scattering of the ejected electron by the nucleus. The theoretical work of Ref [1] predicted that interference effects in the TDCS could be modeled by multiplying the single atom cross section by an “interference factor” of the form

$$I = 1 + \frac{\sin(Q\rho_0)}{Q\rho_0}, \quad (2)$$

where  $Q = k_i - k_a - k_b$ , ( $k_i$ ,  $k_a$ ,  $k_b$ ) are the momenta of the (incident, scattered, ejected) electrons, respectively,  $\rho_0$  is the equilibrium internuclear distance in the target molecule, and  $Q$  is the momentum transferred to the residual ion. For hydrogen molecules an additional factor of 2 is included to account for the two-center nature of  $H_2$  compared with H, and the interference term itself ( $I$ ) has a sinc function behavior as a function of the angle between the ejected electron and the momentum transfer direction. Plots of this factor as a function of the experimental detection angle of the ejected electron, for the experimental conditions used in our measurements, are shown in Fig. 1.

It is important to point out that the cross sections measured in these experiments are not on an absolute scale. Hence a factor of 2 increase in the cross section due to the interference factor, for example, cannot be verified. This was the motivation for using cross section ratios to look for evidence of the effect in previous work on DDCS. Inspection of the interference factor in Fig. 1 for different ejected electron energies shows that the factor is relatively uniform across the angular range corresponding to the recoil region ( $180^\circ$  to  $360^\circ$ ). Hence the measured TDCS (which is on a relative scale) would show essentially no difference in shape in this region, even if interference effects are present. Similarly, the shape of the interference factor in the binary region follows quite closely the shape of the binary peak in the cross section, and hence again the

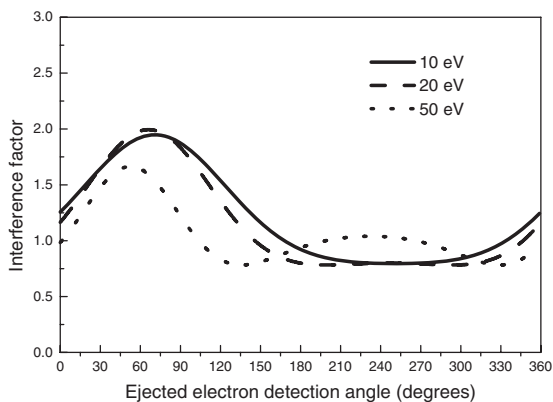


FIG. 1. Interference factor,  $I$ , as a function of ejected electron emission angle, for three different ejected electron energies.

effect of the interference factor in this region alone would be difficult to detect. However, the interference factor changes considerably *between* the binary and recoil regions. Indeed, for an ejected electron energy of 10 eV, Eq. (2) would predict an enhancement of a factor of 2 in the magnitude of the TDCS in the binary region (relative to the recoil region), compared with the single atom case. Depending upon the normalization used, this could manifest itself as a suppression of the recoil peak compared to the binary peak. In this work, we have used a comparison between the shape of the He cross section and the shape of the  $H_2$  cross section to look for such interference effects. The experimental data are compared with full distorted wave calculations for electron impact ionization of He and  $H_2$ ; interference effects should be inherently built in to the latter.

The apparatus used to perform the measurements has been described elsewhere [8]. It comprises an electron gun, and two hemispherical electron energy analysers, the latter being independently rotatable in the scattering plane. The target gas enters the interaction region through a stainless steel capillary, at right angles to the incident electron beam. The two outgoing electrons from the ionization event are detected in time coincidence. One of the hemispherical electron energy analyzers is equipped with a channeltron detector, while the other incorporates a position sensitive detector. Figure 2 shows the binding energy spectra [coincidence count rate as a function of ejected electron energy—the count rate drops off when Eq. (1) is no longer satisfied, within the coincidence energy resolution], plotted as a function of channel number across the position sensitive detector, for  $H_2$  and He ionization. The  $H_2$  binding energy spectrum is broadened, in comparison to He, by the rotational structure of the molecule [9]. The decreasing channel number corresponds to a lower energy of the ejected electron (increasing energy loss). Such a binding energy spectrum is acquired at each energy and for each measured angle of the ejected electrons. The triple (or fully) differential cross section is proportional to the coincidence count rate, measured as the area under the curve.

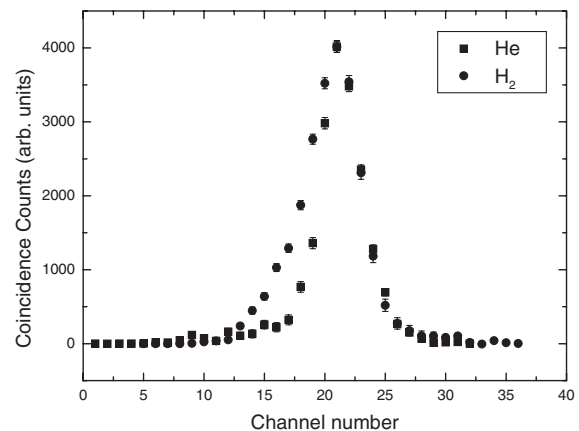


FIG. 2. Binding energy spectrum for He and  $H_2$ .

We also compare the experimental results for both He and H<sub>2</sub> with distorted wave calculations of the fully differential cross section. Here we will present only a brief outline of the theory. More details can be found in [10–13]. We use the 3 distorted wave (3DW) approach for both atomic and molecular ionization. For atomic ionization, the 3DW  $T$  matrix is given by

$$T_{fi}^{3DW} = \langle \mathcal{X}_f \mathcal{X}_{\text{eject}} C_{\text{proj-eject}} | V - U_i | \psi_{\text{active}} \mathcal{X}_i \rangle. \quad (3)$$

Here  $\psi_{\text{active}}$  is the initial bound-state wave function for the active electron,  $\mathcal{X}_i(\mathcal{X}_f)$  is the initial (final) state distorted wave for the projectile electron,  $\mathcal{X}_{\text{eject}}$  is the final-state distorted wave for the ejected electron,  $C_{\text{proj-eject}}$  is the Coulomb interaction between the projectile and ejected electron,  $V$  is the initial state interaction between the projectile and neutral atom, and  $U_i$  is a spherically symmetric approximation for  $V$ .

In the 3DW  $T$  matrix of Eq. (3), the final-state Coulomb interaction between the projectile and ejected electron  $C_{\text{proj-eject}}$  is included in the approximation for the final-state wave function. The important point to note is that any physics included directly in the wave function is included to all orders of perturbation theory so the 3DW has post-collision interaction (PCI) included to all orders of perturbation theory. In contrast, the standard distorted wave approximation does not include this interaction in the final-state wave function which means that PCI is included to first order only. The initial state distorted wave is a solution of the Schrödinger equation

$$\left( T_{\text{proj}} + U_i - \frac{1}{2} k_i^2 \right) \mathcal{X}_i = 0. \quad (4)$$

Here  $T_{\text{proj}}$  is the kinetic energy operator for the projectile,  $U_i$  is the initial state distorting potential, and  $\frac{1}{2} k_i^2$  is the energy of the incident electron. Both final-state distorted waves are solutions of Schrödinger equations similar to Eq. (4) except that the Hartree-Fock atomic neutral potential  $U_i$  is replaced with the Hartree-Fock potential for the final-state ion  $U_{\text{ion}}$ . The final-state distorted waves are orthogonalized to  $\psi_{\text{active}}$  using the Gram-Schmidt procedure. Finally, as described by Prideaux and Madison [10], if the ionization event is treated as a 3-body problem, the perturbation can be approximated as

$$V - U_i = \frac{1}{r_{ab}} - U_{\text{active}}, \quad (5)$$

where  $r_{ab}$  is the distance between the two electrons and  $U_{\text{active}}$  is the spherically symmetric potential for the electron-electron interaction.

The  $T$  matrix for the molecular 3DW (M3DW) approximation is given by

$$T_{fi}^{M3DW} = \langle \mathcal{X}_f \mathcal{X}_{\text{eject}} C_{\text{proj-eject}} | V - U_i | \phi_i^{\text{OA}} \mathcal{X}_i \rangle. \quad (6)$$

The only important difference between the atomic and molecular versions of the 3DW is that the initial atomic wave function for the active electron is replaced with  $\phi_i^{\text{OA}}$

which is the orientation-averaged molecular wave function for the initial bound state of the molecule. Since the experimental measurements for molecules do not distinguish the orientation of the molecule at the time of ionization, the experimental results represent an average over all molecular orientations. In principle, one should calculate the cross sections for each orientation and average the cross sections over all orientations. However in Refs. [12,14] it was shown that it is possible to perform the average over the molecular orientations first for the wave function and then use the orientation-averaged wave function  $\phi_i^{\text{OA}}$  in the calculation of the cross sections. Performing the orientation average first on the wave function instead of on the cross sections represents an enormous savings of computer time. This approximation was shown to be valid for ionization of ground grade states of diatomic molecules if the wave function is dominated by  $s$ -basis sets which is the case for H<sub>2</sub>.

The experimental and theoretical results for the TDCS for He and H<sub>2</sub> ionization are presented in Figs. 3 and 4.

For each ejected electron energy, the cross sections have been normalized at the maximum in the binary region of the cross section. It is interesting to note that, experimen-

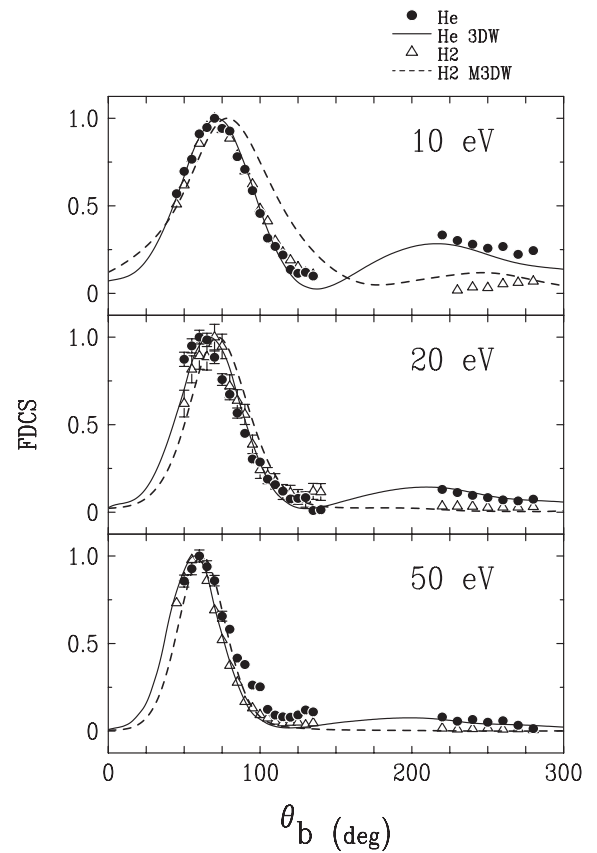


FIG. 3. Experimental (dots and triangles) and calculated fully differential cross sections for He and H<sub>2</sub> at ejected electron energies of 10, 20, and 50 eV, plotted as a function of the emission angle of the ejected electron. See text for a description of the theoretical curves.

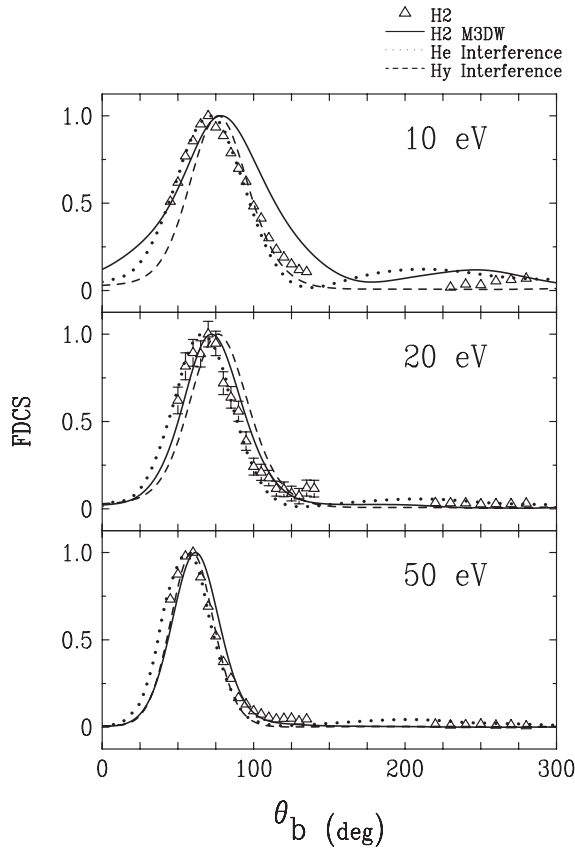


FIG. 4. Experimental (triangles) and calculated fully differential cross sections for  $H_2$  at ejected electron energies of 10, 20, and 50 eV, plotted as a function of the emission angle of the ejected electron. See text for a description of the theoretical curves.

tally and theoretically, the shape of the TDCS near the binary peak is essentially identical for  $H_2$  and He. Figure 3 shows the experimental He and  $H_2$  data, compared with the 3DW results (solid curve) for He; and the M3DW (dashed curve) results for  $H_2$ . At an ejected electron energy of 10 eV, the experimentally determined recoil peak for  $H_2$  is substantially smaller than that for He, and a similar trend is observed for the other ejected electron energies. At all energies the 3DW calculation is in very good agreement with the experimental TDCS for He, while the M3DW generally reproduces the features of the TDCS for  $H_2$ , in particular, the reduced relative size of the recoil peak. Although the M3DW calculation inherently includes interference effects due to the two-center form of the  $H_2$  wave function and distorting potentials, it is not possible to separate out these effects in the calculation.

In Fig. 4, the experimental  $H_2$  data are now compared with the M3DW calculation (solid curve), and the 3DW calculation for He, multiplied by the interference factor (i.e.  $\sigma_{He} * I$ , dotted curve). As can be seen from the figure, the effect of the interference is to reduce the relative size of the He recoil peak, reproducing very well the observed smaller magnitude of the recoil peak in the  $H_2$  cross section. Indeed, in the binary peak region,  $\sigma_{He} * I$  is in

better agreement with the measured  $H_2$  TDCS than is the M3DW calculation. Also shown in Fig. 4 (dashed line) is a calculation of the TDCS for ionization of the hydrogen atom multiplied by the interference term  $\sigma_{Hy} * 2I$ . This is equivalent to the theoretical cross section which was used for comparison in [2,3,5,7]. Interestingly, the latter calculation tends to underestimate the size of the recoil peak compared with  $\sigma_{He} * I$  and the M3DW. Nevertheless,  $\sigma_{Hy} * 2I$  is also in reasonable agreement with the experimental data.

The good agreement between the experimental results, and calculations that include the effect of interference, either explicitly or implicitly, supports the conclusion that the recoil peak for  $H_2$  is suppressed due to the effects of interference, relative to what is observed for the equivalent single center atom. Hence we have shown that interference is directly observable in the angular distributions.

This work was partially supported by the Australian Research Council Centre of Excellence in Antimatter-Matter Studies. M.F., J.G., and D.H.M. would like to acknowledge the support of the U.S. NSF under Grant No. PHY-0456528.

- [1] C. R. Stia, O. A. Fojón, P. F. Weck, J. Hanssen, and R. D. Rivarola, *J. Phys. B* **36**, L257 (2003).
- [2] N. Stolterfoht, B. Sulik, V. Hoffmann, B. Skogvall, J. Y. Chesnel, J. Rangama, F. Frémont, D. Hennecart, A. Cassimi, X. Husson, A. L. Landers, J. A. Tanis, M. E. Galassi, and R. D. Rivarola, *Phys. Rev. Lett.* **87**, 023201 (2001).
- [3] N. Stolterfoht, B. Sulik, B. Skogvall, J. Y. Chesnel, F. Frémont, D. Hennecart, A. Cassimi, L. Adoui, S. Hossain, and J. A. Tanis, *Phys. Rev. A* **69**, 012701 (2004).
- [4] Deepankar Misra, U. Kadhane, Y. P. Singh, L. C. Tribedi, P. D. Fainstein, and P. Richard, *Phys. Rev. Lett.* **92**, 153201 (2004).
- [5] O. Kamalou, J.-Y. Chesnel, D. Martina, J. Hanssen, C. R. Stia, O. A. Fojón, R. D. Rivarola, and F. Frémont, *Phys. Rev. A* **71**, 010702(R) (2005).
- [6] Junfang Gao, D. H. Madison, and J. L. Peacher, *Phys. Rev. A* **72**, 032721 (2005).
- [7] A. J. Murray, *J. Phys. B* **38**, 1999 (2005).
- [8] D. S. Milne-Brownlie, S. J. Cavanagh, Birgit Lohmann, C. Champion, P. A. Hervieux, and J. Hanssen, *Phys. Rev. A* **69**, 032701 (2004).
- [9] K. Jung, E. Schubert, D. A. L. Paul, and H. Ehrhardt, *J. Phys. B* **8**, 1330 (1975).
- [10] A. Prideaux and D. H. Madison, *Phys. Rev. A* **67**, 052710 (2003).
- [11] A. Prideaux, D. H. Madison, and K. Bartschat, *Phys. Rev. A* **72**, 032702 (2005).
- [12] Junfang Gao, D. H. Madison, and J. L. Peacher, *J. Chem. Phys.* **123**, 204314 (2005).
- [13] M. Foster, D. H. Madison, J. L. Peacher, M. Schulz, S. Jones, D. Fischer, R. Moshhammer, and J. Ullrich, *J. Phys. B* **37**, 1 (2004).
- [14] Junfang Gao, D. H. Madison, and J. L. Peacher, *Phys. Rev. A* **72**, 020701(R) (2005).